

A Flexible Blood Flow Phantom Capable of Independently Producing Constant and Pulsatile Flow with a Predictable Spatial Flow Profile for Ultrasound Flow Measurement Validations

Ilmar A. Hein, *Member, IEEE*, and William D. O'Brien, Jr., *Fellow, IEEE*

Abstract—The validation of the ultrasound time-domain correlation method of measuring blood flow has required the development of a flexible blood flow phantom capable of generating predictable flow profiles under a wide variety of conditions. The purpose of the phantom is to generate flow with well-known flow properties and not to mimic actual *in vivo* vessels. This paper describes a flow phantom which can independently generate both constant and pulsatile flow over a wide range of flow rates with a spatially fully developed laminar flow profile. It incorporates a computer-controlled pulsatile pump, which can produce different temporal pulsatile waveforms. The flow phantom also supports multiple vessels, different vessel sizes, as well as different attenuating media. The fluid most commonly used in the phantom is Sephadex mixed with water, and the probability density function of ultrasound reflected from Sephadex is experimentally determined and compared with that of blood. Examples of different constant and pulsatile flow experiments using the phantom are presented.

INTRODUCTION

THE knowledge of the volumetric blood flow rate is an important quantity in the diagnosis of various diseases and trauma as well as in cardiovascular research. A number of different types of instruments are used in medicine to measure blood flow. The use of ultrasound to measure noninvasively blood flow has become a standard clinical practice. The well-known Doppler technique has been in use for many years; and newer methods, such as time-domain correlation, are constantly under development. The electromagnetic blood flowmeter is another common instrument used for measuring blood flow in a surgical setting. An important device, whether it be in the validation of a new flow measurement technique or in the calibration and testing of an existing piece of equipment is a reliable blood flow phantom. It should be able to generate flow rates similar to those found within the human body yet produce repeatable, consistent, and well-under-

stood spatial flow profiles. This paper describes a versatile blood flow phantom system capable of generating both constant and pulsatile flow with a predictable flow profile over a wide range of flow rates.

DESIGN REQUIREMENTS

The blood flow phantom described in this paper was developed to validate the ultrasound time-domain correlation method of measuring blood flow [1], [2]. A phantom was needed which could more realistically simulate flow conditions within the human body yet retain a predictable flow profile within the vessel. The flow velocities and spatial flow profiles of blood flow in the human body can vary greatly, depending on the measurement site, whether it is arterial or venous flow, as well as the state of the vessel (healthy or diseased). In general, blood flow velocities in a normal human adult are in the range of approximately 1 mm/s in small arterioles to 100 cm/s for arteries in the arterial system; and approximately 0.5 mm/s in venules to 40 cm/s in veins for the venous system [3]. The spatial velocity profile in normal arteries is laminar (except near bifurcations) and ranges from a blunt profile to a parabolic profile, depending on the point in the cardiac cycle, as well as the entrance length of the particular vessel [4]. Venous flow is also typically laminar [3]. Pulsatile flow frequencies are determined by the heart rate, and in humans, the maximum heart rate is approximately 180 beat/min [5]. For a normal, resting human, the heart rate rarely exceeds 80–90 beat/min.

The design criterion for the blood flow phantom was to produce flow in vessels with a parabolic, fully developed laminar flow profile over the range of velocities and frequencies normally found in the human body. It was not intended to mimic actual *in vivo* vessels since the flow properties there are not always well understood. The specific goals were as follows: 1) The phantom should be able to produce constant flow with a fully developed laminar flow profile over the range of velocities normally found in the venous system. 2) It should be able to pro-

Manuscript received July 18, 1991; revised April 14, 1992.

The authors are with the Department of Electrical and Computer Engineering, University of Illinois, Urbana, IL 61801.

IEEE Log Number 9203400.

duce pulsatile flow over a frequency and flow velocity range similar to that found in the normal arterial system. The spatial flow profile should be fully developed and laminar and the temporal profile should be variable. 3) The phantom should be able to accommodate different sizes and types of vessels. 4) The spatial orientation of the transducer with respect to the vessel should be accurately and precisely determinable and variable. 5) It should be able to accommodate different attenuating media. 6) It should be easily modifiable to produce any custom-needed transducer/vessel geometry.

A number of different flow phantoms have been described in the literature. Constant flow phantoms can be easily constructed using two reservoirs placed at different heights to create a constant pressure head. The two reservoirs are connected by a vessel and gravity causes fluid to flow from the upper to the lower vessel. A pump is used to return the fluid to the upper reservoir. The vessel in which measurements are to be made can be positioned horizontally as described by Douville *et al.* [6], Voyles *et al.* [7], and Yuan and Shung [8]; however, sedimentation of the fluid may occur and thin-walled vessels such as dialysis tubing may sag in this configuration. Law *et al.* [9] and Embree and O'Brien [2] describe constant flow phantoms with a vertical geometry.

Pulsatile flow has been generated by a number of different means. Douville *et al.* [6], Tortoli *et al.* [10], and Lavandier *et al.* [11] have used a roller pump to produce pulsatile flow. This type of pump generates flow by squeezing a plastic tube against a fixed wall and forcing fluid in one direction in a pulsatile manner. This method produces pulsatile flow but it is not very controllable. Law *et al.* [12] have used a computer-controlled roller pump to produce a wide variety of waveforms. Computer-controlled gear pumps have been used by Peterson [13], McDicken [14], and Hoskins *et al.* [15]. A problem with gear pumps, however, is that damage to scattering particles in the fluid may occur due to the grinding action of the gears. Phantoms based on piston pumps have been described by Werneck *et al.* [16], Poots *et al.* [17], Shortland and Cochrane [18], and Holdsworth *et al.* [19].

One limitation of the pulsatile pumping systems listed above is that they cannot independently produce constant flow, which is a requirement of the desired flow phantom. Lavandier *et al.* [11] have used two roller pumps; one for continuous and one for pulsatile flow. The problem with using roller pumps for continuous flow is that undesirable small pulsatile components may exist due to the nature of the roller pump. Giddens and Khalifa [20] and Ku *et al.* [21] have constructed systems incorporating the constant pressure head of the constant flow phantoms along with a computer-controlled spool valve which can redirect flow into different tubes to produce pulsatile flow in the measurement vessel. This approach adds complexity to the phantom since extra bypass tubes are required.

Many of the phantoms described in the literature fulfill some of the requirements of the desired phantom; however, a number of features, such as ability to incorporate

multiple vessels and vessel sizes, as well as topics such as the spatial profile of the pulsatile flow have not been found. The current blood flow phantom system is the result of a number of years of modification and revision and has been used to validate the ultrasound time-domain correlation (UTDC) technique under pulsatile conditions [22] as well as studies with vessels with obstructions [23], and with different size vessels and multiple vessels [24].

MATERIALS AND METHODS

Fig. 1 illustrates the current blood flow phantom system. It is a modification of the one used by Embree and O'Brien [2] to validate the UTDC technique under constant flow conditions and was only capable of producing constant flow. The current phantom consists of two pumping systems (a peristaltic pump and a syringe pump) and a measurement fixture. The different components of the phantom are connected by polyethylene tubing (Fisherbrand 1/4" inner diameter, 1/16" wall thickness) and are placed in a temperature-controlled water bath (Excal model EX-500). The transducer is submerged in the bath, which provides a water path to the measurement vessel. Transducers or scanheads which are not waterproof can be placed in a plastic bag along with coupling gel and then submerged.

Constant Flow Generation

The peristaltic pump (Masterflex model 7520) is used to establish constant flow. The constant flow rate is set by adjusting the height H between the upper and lower reservoirs. Gravity causes fluid to flow from the upper reservoir through the vessel to the lower reservoir, and from there to the return reservoir. The peristaltic pump moves the fluid back to the upper reservoir. The fluid is pumped from the bottom of the return reservoir to help keep the blood or blood mimicking substance mixed. Constant laminar flow in the vessel is given by [25]

$$Q = \frac{D^4 g \rho_0 H}{128 \mu L} \quad (1)$$

where Q is the volumetric flow rate (m^3/s), D is the vessel diameter (m), g is the acceleration due to gravity (9.8 m/s^2), ρ_0 is the fluid density (1000 kg/m^3 for water), H is the head loss (m), μ is the fluid viscosity ($0.001 \text{ N}\cdot\text{s/m}^2$ for water), and L is the total tube length between the upper and lower reservoir (m). For a 6.5 mm diameter tube with a tube length of 2.3 m and a head loss of 8.4 cm, a 300 mL/min flow rate is produced.

The measurement fixture has a built in minimum entrance length E from the top of the fixture to the ultrasonic measurement point. The minimum entrance length determines the flow rates over which fully developed parabolic laminar flow is established and is given by [25]

$$E = 0.073 \rho_0 Q / \mu. \quad (2)$$

The vessel fixture has a 35 cm entrance length which guarantees the spatial flow profile to be fully developed

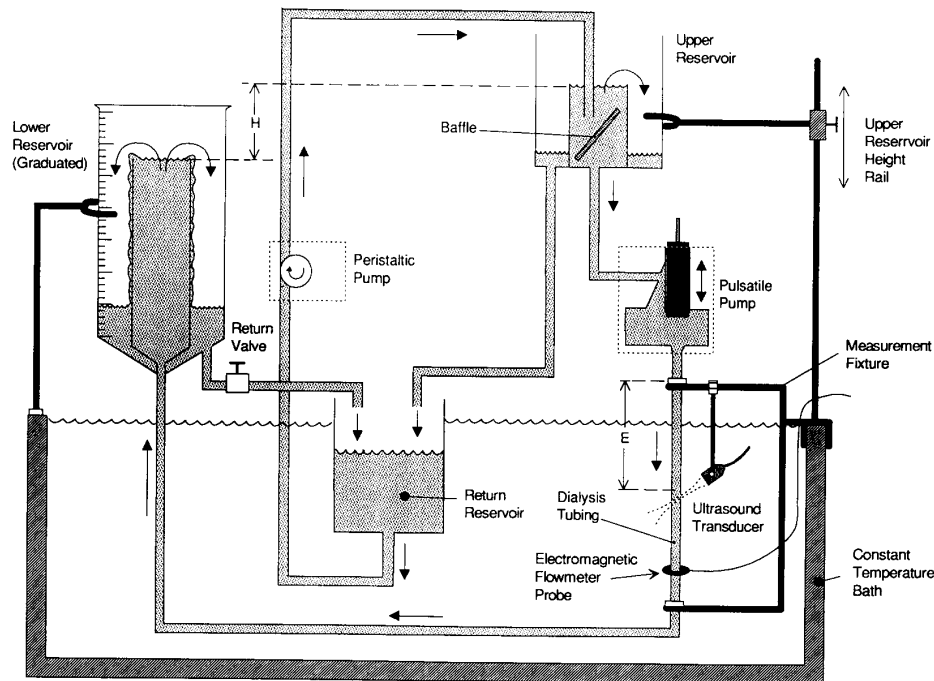


Fig. 1. Blood flow phantom system. Continuous flow is produced by the constant pressure head between the lower and upper reservoir. Independent pulsatile flow is generated by a piston-based pulsatile pump placed between the upper reservoir and measurement fixture.

and laminar for volumetric flow rates up to 300 mL/min (for a 6.5 mm diameter vessel). In addition to the built in minimum entrance length of the vessel fixture, a 30 cm section of polyethylene tube connects the vessel fixture to the pulsatile pump. This section increases the effective minimum entrance length and increases the effective range of fully developed laminar flow to 530 mL/min. In practice, the flow profiles appear to be parabolic to 1000 mL/min. Longer sections of tube can be added to increase the minimum entrance length.

The constant flow rate can be measured independently (nonultrasonically) by measuring the time it takes for a known volume to be filled with fluid. The lower reservoir in the phantom is a 1 L graduated Pyrex® glass cylinder and is used for this purpose (see Fig. 1). The graduated cylinder is 6.0 cm in diameter and 45.0 cm long. It has been modified by a glass blower by placing a 4.0 cm diameter 39.0 cm long glass cylinder within the graduated cylinder along with two openings at the bottom fitted for 1/4" polyethylene tubing. The inner cylinder and openings have been placed in the graduated cylinder such that fluid will enter from the bottom, fill the inner cylinder, and then overflow into the volume between the inner cylinder and the graduated cylinder. When the return valve is open, the flow continues out the graduated cylinder and into the return reservoir and the fluid level in the inter-cylinder volume remains constant. When the return valve is closed, the inter-cylinder volume will fill up at a rate

dependent on the volumetric flow. The graduations on the graduated cylinder have been recalibrated to represent the inter-cylinder volumes. The inter-cylinder volume as calibrated to the 1 L mark is 356.0 mL. The time it takes to fill this volume can be measured with an uncertainty of approximately ± 0.5 s; thus a 500 mL/min volumetric flow rate can be measured with an accuracy of $\pm 1.2\%$. This method of measuring the flow is referred to as the *hydrodynamic flow rate* and is the reference flow rate used to assess the accuracy of ultrasonic measurements with constant flow.

The range of constant volumetric flows which can be produced in a 6.5 mm diameter dialysis tube with this system is from approximately 2.5 to 750 mL/min, which corresponds to flow velocities in the range of 2.5 mm/s to 75 cm/s.

Pulsatile Flow Generation

Poots *et al.* [17] have shown that pulsatile flow with a spatially laminar profile can be produced for positive flows within a phantom. If the instantaneous volumetric flow rate is always positive and less than the maximum fully developed flow rate as determined by the minimum entrance length [see (2)], the spatial flow velocity profile should always be fully developed and laminar. The instantaneous flow rate will be positive at all points if the constant flow component is adjusted high enough, and the

effective minimum entrance length can be increased for high flow rates produced by pulsing flow.

Pulsatile flow is generated by a piston-based pumping system, which is located between the upper reservoir and the measurement fixture. When the pulsatile pump is off, only constant, nontime varying flow is present. When the pulsatile pump is on, a peak-to-peak flow component oscillates around an average flow component. Fig. 2 illustrates the pulsatile pumping system. The heart of the system is a pulsing unit which consists of a fluid chamber (90 mL volume) and a modified commercially available syringe (20 cc, American Hospital Supply Corporation). The unit is a custom molded Plexiglas® block into which the fluid chamber, fluid flow passages, and syringe shape have been bored. One quarter inch brass hose connectors (Peoria Valve and Fitting) are used to interface fluid flow from external tubes into the pulsing unit. These connectors are threaded at one end and barbed at the other, and are threaded into the Plexiglas® block. The syringe has been modified by removing the needle and top such that the plunger can move in and out of the fluid chamber. The continuous flow component enters the pulsing unit near the top, passes through the fluid chamber, and then passes out the bottom to the dialysis tubing. The motion of the syringe is produced by a stepper motor (Superior Electric type MO61-FD02, rated at 5 V 1 A, 200 steps/rev) controlled by a PC (with Metrabyte MSTEP-5 stepper motor control board). A gearbox translates the circular motion of the stepper motor to the translational back-and-forth motion of the syringe. One revolution of the stepper motor produces a ± 0.5 cm displacement of the syringe plunger, which corresponds to a ± 1.4 mL volumetric displacement. This may seem like a rather small volumetric displacement; however, it must be remembered that the volumetric flow rate is proportional to the derivative of the displacement. If the volumetric displacement of the syringe is given by $1.4 \sin(\omega t)$ mL, for example, the volumetric flow rate Q would be

$$Q = 1.4 \omega \cos(\omega t) \text{ mL/s.} \quad (3)$$

For a pulsatile frequency of 150 beat/min, this would produce pulsatile volumetric flow rates of 1.3 L/min. In practice, pulsatile flow rates this high are not seen in the phantom due to the impedances of the vessels; an electrical circuit and analysis of the flows produced in the phantom is presented in the next section.

The frequency of pulsation and the temporal pulsatile waveform is controlled by a personal computer. The stepper motor can be programmed via the PC to produce various types of time-varying flow profiles. The frequency of pulsing is measured independently by an infrared optical detector (Honeywell HOA-2001) mounted to the translational shaft of the gearbox. The shaft interrupts the infrared beam in the optical detector whenever the syringe is pulled all the way back, which happens once every pulse. The pulsatile period counter then displays the time between pulses.

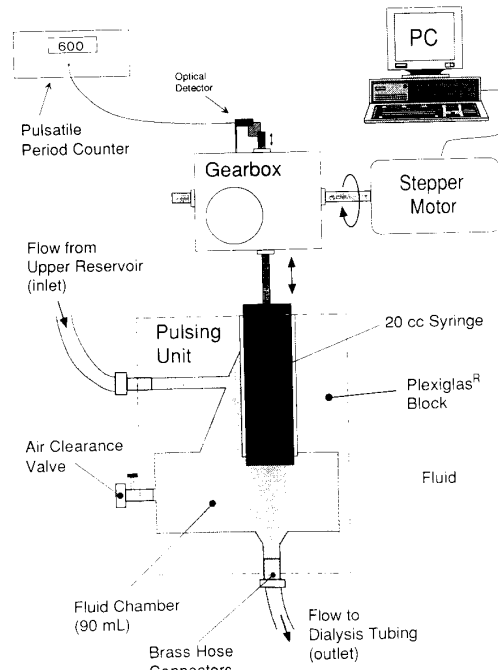


Fig. 2. The pulsatile pump system consists of a piston moved in and out of a chamber. The volume displacement is adjusted in the gearbox and the pulsing waveform is controlled by the stepper motor/computer.

Electrical Circuit Equivalents

A simple equivalent electrical circuit for the phantom is shown in Fig. 3 for constant and pulsatile flow. The blood flow phantom can be modeled with an equivalent electrical circuit comprising four basic sections: 1) the pressure head used to generate constant flow, 2) the pulsatile pump, 3) the section of tubing connecting the upper reservoir to the pulsatile pump [upper tubing in Fig. 3(a)], and 4) everything from the pulsatile pump to the lower reservoir, which includes the tube from the pulsatile pump to the measurement fixture, the vessel in the measurement fixture, and the tube from the measurement fixture to the lower reservoir [lower tubing in Fig. 3(a)]. The constant pressure head can be modeled as a constant voltage source H and the pulsatile pump as a time-varying current source $Q_p(t)$ with a shunt resistance R_p . The tubing in the phantom can be modeled as having resistance R corresponding to steady flow resistance, inductance L corresponding to inertia of the fluid, and capacitance C corresponding to effects of vessel wall elasticity [3]. The polyethylene tubing connecting different parts of the phantom is thick and rigid and is considered to have no capacitance for the frequencies used. The upper tubing section is short (compared to the lower tubing) and consists only of polyethylene tubing; hence its impedance (Z_U) consists only of a resistive and inductive components R_U and L_U . The measurement vessel used most frequently in the measurement fixture is dialysis tubing, which is very thin and elastic and changes diameter for pulsatile flow. Thus the impedance of the lower tubing section (Z_L) is modeled as having

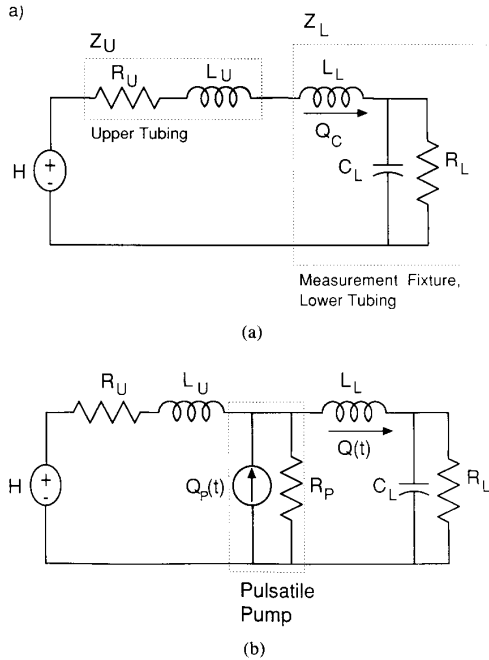


Fig. 3. Electrical circuit equivalent of the blood flow phantom for (a) constant flow and (b) pulsatile flow. The resistors represent resistance of the vessel to constant flow, the inductors represent the inertia and momentum of the fluid, and the capacitor represents the behavior of an elastic wall.

resistive, inductive, and capacitive components R_L , L_L , and C_L , respectively.

The electrical circuit model for only constant flow is shown in Fig. 3(a). For constant flow, once steady state has been achieved, the inductors are effectively short circuits and the capacitor an open circuit, and the constant flow rate Q_c is given by

$$Q_c = H / (R_U + R_L). \quad (4)$$

The activation of the pulsatile pump causes the current source $Q_p(t)$ with shunt resistance R_P to be placed in parallel into the circuit, as shown in Fig. 3(b). The total flow rate $Q(t)$ passing through the vessel in the measurement fixture can be expressed as

$$Q(t) = Q_{dc} + Q_{ac}(t) \quad (5)$$

where Q_{dc} represents the average dc component of flow and Q_{ac} represents the time-varying ac component of flow. Q_{dc} is given by

$$Q_{dc} = \frac{HR_P}{R_L R_U + R_L R_P + R_U R_P} \quad (6)$$

The ac component $Q_{ac}(t)$ can be determined by solving the second-order differential equation

$$A \frac{dQ_p(t)}{dt} + B = C \frac{d^2 Q(t)}{dt} + D \frac{dQ(t)}{dt} + E \quad (7)$$

where the constants A through E are determined by R_U , R_P , R_L , L_U , L_L , and C_L .

The equivalent impedances and resistances used in the circuit model are dependent on factors such as the tube lengths, diameters, and bends; the type and number of vessels in the vessel fixture; the vessel wall elasticity; and the fluid viscosity, which are difficult and not practical to estimate. In practice, the blood flow phantom is set up for a particular configuration and the height rail is calibrated for constant flow by setting different heights and measuring the hydrodynamic flow with the pulsatile pump off. Pulsatile flow is set by adjusting the constant flow high enough such that the total flow $Q(t)$ is always above zero after the pulsatile pump is activated. An example of the resulting pulsatile flow a dialysis tube for a given constant flow rate and pulsatile pump waveform is given in the results section of this paper.

Pulsatile flows with peak volumetric flow rates of 1.1 L/min at frequencies up to 150 beat/min, with corresponding flow velocities of 1 m/s, have been produced with this pulsatile flow system. Volumetric pulsatile flow in the phantom is measured independently with an electromagnetic (EM) flowmeter (Zepeda Instruments SWF-5RD). The output from the EM flowmeter is digitized, stored, and displayed by a PC. The EM flowmeter is calibrated under constant flow conditions at the maximum and minimum flow peaks for each pulsatile experiment. This procedure consists of obtaining and storing a pulsatile flow trace, after which the pulsatile pump is turned off. The constant flow is then adjusted until the constant flow trace equals the minimum peak level of the stored pulsatile flow trace, and again at the maximum peak level of the stored trace. The reported accuracy of the Zepeda Instruments EM flowmeter is $\pm 3.0\%$ [26].

Measurement Fixture

Fig. 4 illustrates the measurement fixture. The measurement fixture consists of two components, a vessel fixture and a transducer mounting assembly.

1) *Vessel Fixture*: The vessel fixture consists of a series of poly connector adapters mounted on a metal support bracket. The poly connectors are available in different sizes and adapt the phantom polyethylene tubing to the vessel diameter in the vessel fixture. For thin-walled vessels, such as dialysis tubing, a small section of polyethylene tubing is used to hold the dialysis tubing in place against the poly connector.

Different attenuating media can be attached to the support bracket and made to surround the vessel within the vessel fixture. Tissue samples with different ultrasonic attenuation properties, such as liver and spleen, have been used to surround the dialysis tube to investigate the effects of ultrasonic attenuation on the UTDC technique [23]. Other materials less prone to decomposition, such as natural sponge, have also been used.

Since blood vessels frequently come in pairs in the body, the vessel fixture was made to support more than one vessel. The phantom can currently support two vessels, which can be different sizes and have different flow

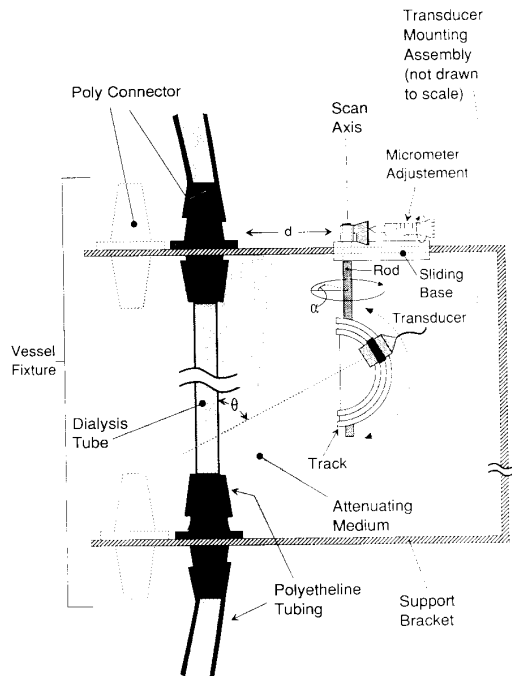


Fig. 4. The measurement fixture consists of a vessel fixture and a transducer mounting assembly. The vessel fixture can accommodate different sizes and types of vessels via the poly connector adapters. The transducer mounting assembly can precisely orient the transducer with the vessel. Different types of attenuating media can be placed in the fixture to surround the vessel.

rates and directions (the flow in one vessel can be made to move in the opposite direction as in the other vessel).

2) *Transducer Mounting Assembly*: The transducer mounting assembly allows exact spatial alignment of the transducer with respect to the vessel. The ultrasonic measurement angle θ , the scan angle α , and the distance d can all be adjusted precisely. The measurement angle θ is the angle between the ultrasound beam axis and the vessel (also called the Doppler angle). The scan angle α describes the rotational position of the transducer on the scan axis. α determines the point where the ultrasound beam intersects the vessel where $\alpha = 0$ corresponds to the beam passing through the center of the vessel. The two-dimensional flow velocity profile across the vessel can be sampled by varying α . The distance d is the distance the measurement fixture is located from the vessel and can be used to vary the distance of the transducer from the vessel.

The transducer mounting assembly is constructed on a sliding base (see Fig. 4), which can slide back and forth along the support bracket to vary the distance d . This distance can be adjusted to an accuracy of approximately ± 0.25 mm. The transducer itself is mounted on a calibrated circular track. The measurement angle θ can be varied by changing the location of the transducer on the circular track [2]. The measurement angle can be adjusted with an accuracy of approximately $\pm 0.5^\circ$. The track is connected by a circular rod to the sliding base. The rod defines the scan axis about which α is varied. The rod is

spring-loaded, and a micrometer adjustment is used to vary α with an accuracy of approximately $\pm 0.016^\circ$ [2].

Blood Mimicking Fluid

A number of different recipes have been described in the literature for blood mimicking fluids used in flow phantoms [9]. For this phantom, a blood-mimicking fluid which has statistical properties similar to that of blood is required. The size of erythrocytes is on the order of 5–7 μm [27] and meets the criterion for a Rayleigh scatterer ($r \ll \lambda$) in the 1–10 MHz ultrasonic frequency range. The number of scattering erythrocytes in blood is large enough such that the backscattered ultrasonic signal can be described as a Gaussian random process [28], [29]. Sephadex particles in various concentrations have been used in water [6], [10] as well as in a glycerine-water mixture [30]. Sephadex is a desirable blood substitute since it is easy to mix and will not degrade with time. The Sephadex particle size (20–80 μm diameter) is larger than erythrocytes but is still small enough to be considered a Rayleigh scatterer at 5 MHz. The power reflected by Sephadex particles is dependent on the concentration [30] and can be adjusted to approximately match the power reflected by blood. The probability density function and reflected power of Sephadex have been experimentally determined and compared with human blood in Fig. 5. The Sephadex concentration is 2.0 g/L in deionized water and was flowing at a rate of 400 mL/min in a 6.5 mm diameter vessel. The vessel was imaged at 5 MHz and ultrasonic echo signals from flow within the vessel were digitized and stored (the data acquisition system is described in detail in [24]). The A/D input range was -0.5 to $+0.5$ V and RF echo signals were digitized at 50 MHz with an 8-bit word length. The 8-bit word provides 256 possible values between -0.5 and $+0.5$ V. The normalized probability has been calculated by plotting the number of times each discrete value has occurred (for 100 000 samples) and the area under the curve has been normalized to one. The normalized received ultrasonic power has been calculated from the digitized echo signals by measuring the total received power in all the samples divided by the number of samples (100 000). The theoretical Gaussian curve (calculated with the measured mean and standard deviation of the echo signals from the moving Sephadex fluid) has been superimposed on the experimental data. As a comparison, the probability density function of flowing blood in a normal human carotid artery has been measured and plotted in Fig. 5(b). The transmitted power levels and distances from the transducer were identical for both the blood and Sephadex measurements. Both the blood and the Sephadex reflect ultrasound with approximately a Gaussian distribution, and the received ultrasonic signal power from both is on the same order of magnitude. For these reasons a 2.0 g/L concentration of Sephadex has been chosen as the blood mimicking substance in the phantom. For constant flow experiments the distilled water-Sephadex mixture is used; for pulsatile experiments, a normal saline-Sephadex mixture must be used

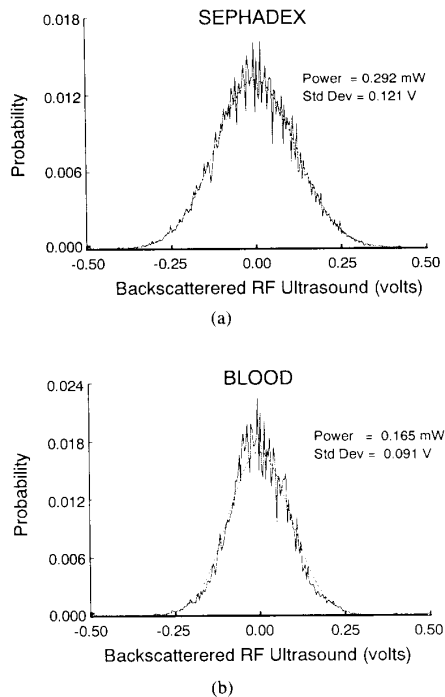


Fig. 5. Probability density function experimentally determined for (a) 2.0 g/L Sephadex particles in water and (b) human blood flow in a normal carotid artery. The theoretical Gaussian curve generated from the mean and standard deviation of the echoes has been superimposed on the experimentally determined PDF's.

because the EM flowmeter requires the fluid to be conductive [26]. For specialized experiments, glycerine-based fluid and porcine blood have also been used in the phantom [2].

RESULTS

Constant Flow Profiles

1) *A Single Vessel*: Fig. 6 shows a long axis ultrasound image of a 6.5 mm diameter dialysis tube surrounded by a natural sea wool sponge (#10414, Acme Sponge and Chamois Co., Tarpon Springs, FL) in the flow phantom. The flow through the vessel is constant and the hydrodynamic volumetric flow rate is 300 mL/min. Fig. 7 shows a three-dimensional profile of the flow within the vessel as measured by the UTDC technique. The horizontal axes represent distances from the transducer and the vertical axis represents velocity. The transducer was located at position $x, y = 0, 0$ cm and the vessel was scanned by varying α from -7.0° to $+7.0^\circ$ in 0.5° steps, where $\alpha = 0.0^\circ$ corresponds to the y -axis. The acquired velocity data were converted from polar to rectangular coordinates to produce the three-dimensional plot. Flow velocity profiles were found to be parabolic in shape to hydrodynamic flow rates of 1000 mL/min. An analysis of flow profiles was performed by fitting a theoretical parabolic curve to the measured velocity points and calculating the mean-squared error between the two. The mean-squared error

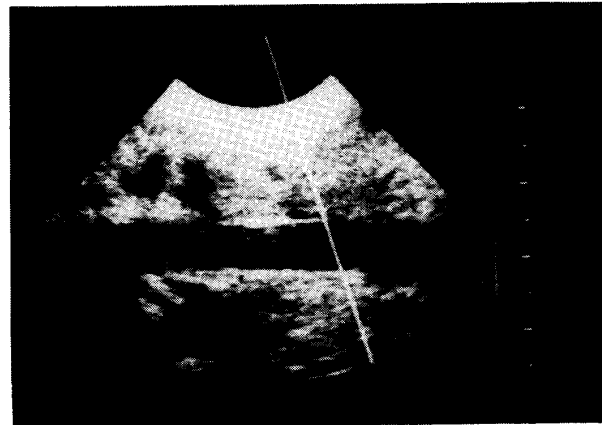


Fig. 6. Long-axis ultrasound image of a 6.5 mm dialysis tube in the blood flow phantom. The dialysis tube is surrounded by natural sea wool sponge and the volumetric flow through the tube is 300 mL/min.

was found to be less than 3% for volumetric flow rates up to 1000 mL/min.

Nonparabolic flow velocity profiles can also be generated within the phantom by adjusting the volumetric flow and entrance length. One-dimensional flow velocity versus range profiles are shown in Fig. 8 for a high flow rate case (solid line) and a small entrance length case (dashed line), along with a normal parabolic flow case (dotted line). The solid line shows the flow velocity profile at 1100 mL/min, with the standard entrance length of 35 cm plus 30 cm of connecting tube to the upper reservoir. Here the entrance length is insufficient for fully developed laminar flow and the top of the flow velocity profile has become blunted.

The dashed line shows a 600 mL/min flow velocity profile when the total entrance length is much shorter, approximately 8 cm plus 16 cm of connecting tube. In this case the flow profile is flat and rough when compared to the normal case (dotted line). This type of turbulent flow profile is typically found near the inlet to a pipe, which in this case is the inlet from the upper reservoir.

2) *Two Vessels*: Fig. 9 shows the three-dimensional flow profile for two 6.5 mm dialysis tubes placed next to each other in the vessel fixture. Unidirectional flow was generated in the two vessels by using a plastic Y -adapter to split the flow coming from the single polyethylene tube into the two vessels. The distance between the Y -junction and measurement point was 35 cm of dialysis tube (corresponding to the entrance length) plus 15 cm of connecting tube. The volumetric flow rate through the left vessel is 384 mL/min and the flow in the right vessel is 298 mL/min (as determined by UTDC). The flow profile is parabolic in shape for both vessels.

Bidirectional flow can also be generated, as shown in Fig. 10. In this case, a horizontal measurement configuration was used to keep the effective resistances in both vessels the same. In a vertical configuration, flow in one vessel would have to move upwards against gravity, in addition to requiring longer connecting tubes. The di-

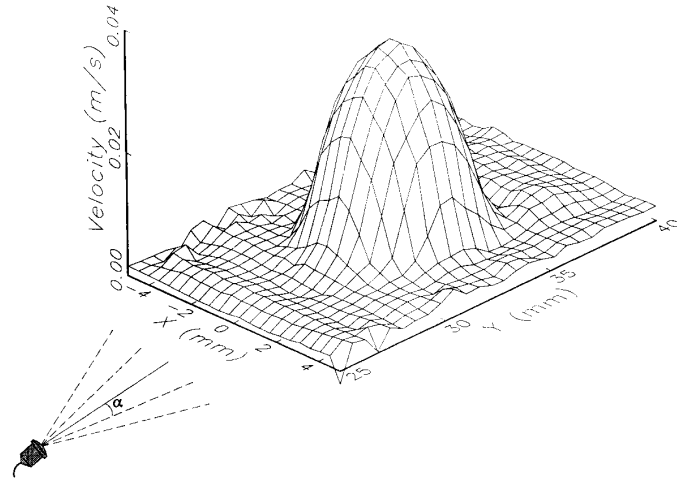


Fig. 7. Three-dimensional profile of the velocity distribution in a 6.5 mm diameter dialysis tube. The transducer was located at position $x, y = 0, 0$ and α was varied from $+7.0^\circ$ to -7.0° in 0.5° steps, where $\alpha = 0$ corresponds to the y -axis. The volumetric flow is fully developed and laminar. The velocity profiles were found to be parabolic in shape to 1000 mL/min.

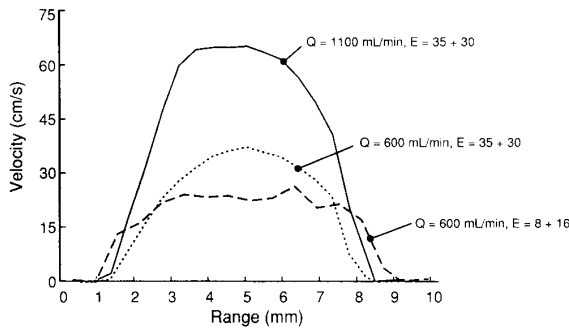


Fig. 8. Flow velocity profiles in a 6.5 mm diameter tube at a high flow rate of 1100 mL/min (solid line), at a flow rate of 600 mL/min with a small entrance length (dashed line), and at 600 mL/min with the standard entrance length (dotted line). The total entrance length E is given as a sum of the entrance length in the measurement fixture along with the length of connecting tube. The range represents distance from the beginning of data acquisition, which physically is at the focal region of the transducer (3 cm from the transducer face).

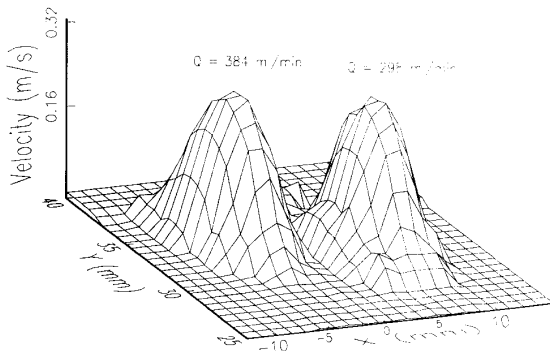


Fig. 9. Three-dimensional velocity profile of flow through two vessels placed next to each other. The flow from the upper reservoir was split using a Y-adapter.

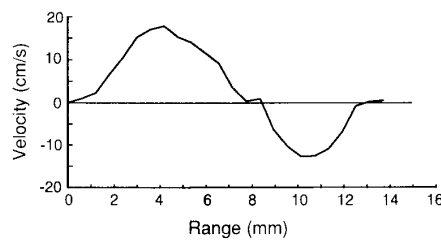
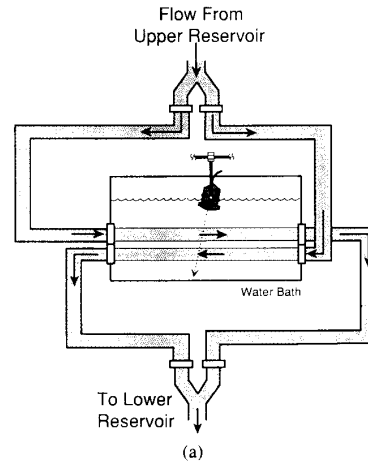


Fig. 10. Bidirectional flow generation in two adjacent dialysis tubes. (a) Phantom set up. The top tube has a diameter of 6.5 mm; the bottom 3.5 mm. (b) Flow velocity profiles in the vessels. A negative flow velocity corresponds to motion away from the transducer.

alysis tubes were mounted into a Plexiglas® water bath, and the polyethylene connecting tubes were equal in length and routed as shown in Fig. 10(a). The transducer mounting assembly was modified such that it could be

placed in a horizontal position. The entrance length for each vessel is at opposite ends of the bath, and was approximately 35 cm for each.

The flow velocity profile (as measured by UTDC) for constant flow within a 6.5 mm and a 3.2 mm vessel was located at the top position and the flow direction was towards the transducer; the 3.2 mm vessel was at the bottom position and flow was away from the transducer. Negative flow velocity in this case corresponds to flow moving away from the transducer. The flow rate in the 3.2 mm vessel was -77 mL/m and the flow in the 6.5 mm vessel was 245 mL/m. The flow profile is parabolic in shape for both vessels.

3) *Partially Obstructed Vessel*: In the real-life situation the blood vessel shape may not be round or there may be obstructions in the vessel. A simple way of producing a partial obstruction in the phantom is to place a wire on one side of the dialysis tube as shown in Fig. 11. The obstruction used was a 3 mm diameter wire which was placed at the far side of the vessel (with respect to the transducer) and spanned the length of the dialysis tubing. This type of obstruction should still produce laminar flow but will change the distribution of flow within the vessel (it will no longer be axially symmetric and may not be parabolic). Fig. 12 shows the three-dimensional flow velocity profile for the partially obstructed vessel. The hydrodynamic volumetric flow rate is 100 mL/min. This plot shows that the one-dimensional flow velocity profiles remain somewhat parabolic as the vessel is scanned from left to right (grid lines running parallel to the y-axis). This type of obstruction produces nonturbulent parabolic flow profiles; turbulent flow in the phantom can be generated by simply constricting the dialysis tubing at the measurement location.

4) *1.5 mm Diameter Vessel*: Vessels other than 6.5 mm diameter dialysis tubes have been used experimentally. The smallest vessel that has been used in the phantom is 1.5 mm inner diameter polyethylene tube. The polyethylene tube is quite small compared to the 6.5 mm diameter dialysis tube; and thus has a proportionally higher resistance to flow. In order to facilitate flow through a tube this small, the 1.5 mm polyethylene tube was connected directly to the upper reservoir and allowed to drain into a 100 mL graduated cylinder instead of requiring the flow to push up into the lower reservoir (see Fig. 1). This also allows the pressure head H to be increased considerably, since it is not limited by the top of the lower reservoir. The outflow from the bottom of the 1.5 mm tube was submerged in fluid in the graduated cylinder (if the tube is not submerged, the flow drips out of the tube, creating somewhat of a pulsatile effect) and the hydrodynamic flow estimated from the filling of the graduated cylinder. The volumetric flow generated through the 1.5 mm diameter tube is relatively small compared to flow in the 6.5 mm diameter dialysis tube; an $H = 127$ cm produced a constant flow rate of approximately 5 mL/min. Thus, it takes approximately 20 min for the graduated cylinder

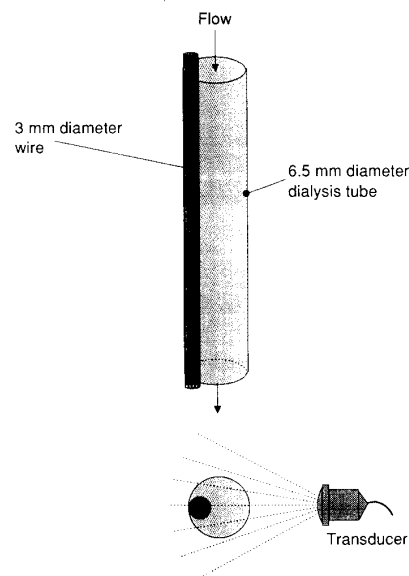


Fig. 11. Obstruction setup and transducer scanning configuration. A partial obstruction of the vessel can be made by placing a 3.0 mm diameter wire on one side of the vessel. This type of obstruction will produce non-axially symmetric flow without turbulence.

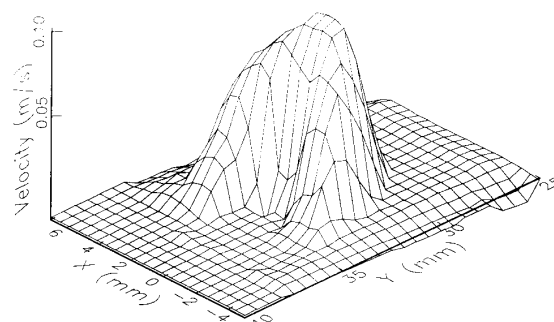


Fig. 12. Three-dimensional velocity distribution of flow within a partially obstructed vessel. The flow profile is no longer axially symmetric but one dimensional profiles along the A -lines remain somewhat parabolic around the obstruction.

to fill, at which time the fluid in the cylinder was manually drained into the return reservoir.

Fig. 13 shows the one-dimensional flow velocity profile along a single A -line through the center of the vessel. The axial velocity resolution for this scan is 0.15 mm and the velocities are nearly uniform across the vessel, indicating that the Sephadex-water mixture has a high degree of plug flow for a vessel this small.

Pulsatile Flow Waveforms

Fig. 14 shows an example of a typical pulsatile flow configuration. Fig. 14(a) shows the velocity of the syringe piston versus time for sinusoidal motion of the piston at a frequency of 100 beat/min. Also shown is the calculated volumetric flows (± 880 mL/min) generated within the pump at the peak piston velocities. The constant hy-

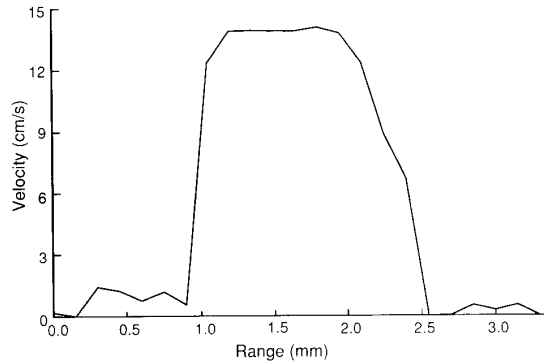


Fig. 13. One-dimensional velocity profile of dripping flow within a 1.5 mm diameter polyethylene tube. The profile was measured along a single *A*-line through the center of the vessel and has a plug flow shape.

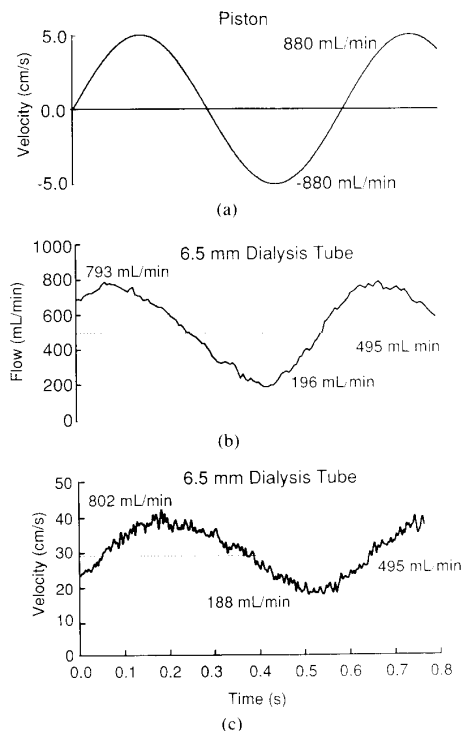


Fig. 14. Pulsatile flow induced in a 6.5 mm diameter dialysis tube in response to sinusoidal motion of the pulsatile pump. The constant flow rate was adjusted to 600 mL/min before activation of the pulsatile pump. (a) Velocity versus time of the syringe piston at a frequency of 100 beat/min after activation of the pulsatile pump. (b) Volumetric flow measured by the EM flowmeter in the dialysis tube. (c) Flow velocity measured at the center of the vessel by UTDC.

hydrodynamic flow rate was set at 650 mL/min before the pulsatile pump was activated. The resulting volumetric flow rates and flow velocities produced in a 6.5 mm dialysis tube after the pump is activated is shown in Fig. 14(b) and (c). The EM flowmeter can measure only the average flow passing through the probe cross sectional area; hence this has been used to show the total volumet-

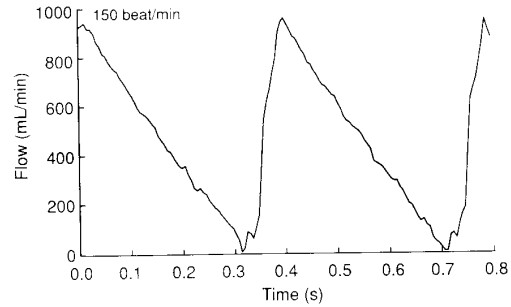


Fig. 15. Temporal flow profile for a 150 beat/min ramp waveform. The constant flow component is adjusted such that instantaneous flow rates are always positive.

ric flow rate versus time in Fig. 14(b). The UTDC flowmeter can measure the average velocity in a small range volume (0.6 mm in diameter and 0.6 mm long) and this has been used to measure the flow velocity at the center of the vessel. The EM and UTDC flowmeter measurements are not exactly in phase since the measurement point in the vessel was slightly different (the EM probe would interfere with the UTDC measurement at the same point). Both measurements show that for input values of 650 mL/min constant flow and 880 mL/min 100 beat/min sinusoidal pulsatile flow, the resulting temporal flow waveform in the dialysis tube consists of a pulsatile flow component with amplitude 300 mL/min oscillating around an average flow component of 495 mL/min. In addition, the waveform is not purely sinusoidal; the time from the maximum peak to minimum peak is approximately 0.32 s and from minimum to maximum is 0.25 s. This distortion is due most likely to the impedances of the vessels, and that the flow acceleration in one direction is aided by the constant flow rate and opposed in the other.

As an example of different temporal waveforms, Fig. 15 shows the volumetric flow versus time as measured by the EM flowmeter for a ramp waveform at 150 beat/min. The spatial flow velocity profile along a single *A*-line through the center of the vessel is shown at the maximum and minimum flow peak for a 120 beat/min ramp waveform in Fig. 16. It shows the flow velocity profiles are approximately parabolic (within 3% mean-squared error of a true parabola) at both peaks and also shows that the diameter of the dialysis tube changes. The dialysis tube is very elastic compared to the connecting polyethylene tubing and changes diameter with the flow rate; expanding to a maximum at the maximum flow peak and contracting to a minimum at the minimum flow peak. The points of symmetry of the minimum and maximum peak profiles are slightly different, most likely due to motion of the tube induced by the pulsatile flow.

A number of investigators have used computer-controlled pumps to produce physiological flow waveforms in phantoms [12], [15], [18], [19]. Future application of the stepper-motor pulsatile pumping system is to integrate it with an *A/D* and an *in vivo* blood flow measurement

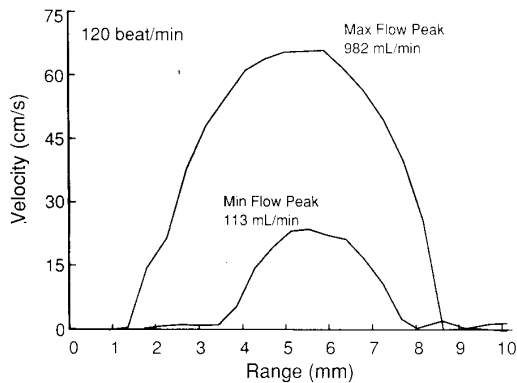


Fig. 16. One-dimensional velocity profiles of flow at the maximum and minimum flow peaks of a 120 beat/min ramp waveform. The dialysis tube is flexible and changes diameter with the pulsing of the flow. The flow profiles are approximately parabolic at both peaks.

system. If the blood flow in a vessel in the human body can be digitized and stored, the stored blood flow waveform can be "played back" (with appropriate software) in the blood flow phantom system.

CONCLUSION

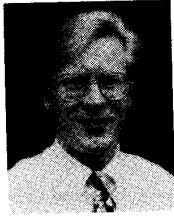
This blood flow phantom system has proven to be indispensable in the validation of the UTDC blood flow measurement technique. It has allowed the measurement system to be tested under a wide range of conditions: for varying flow rates, vessel sizes, transducer orientations, and attenuating media. It can be easily custom configured for almost any type of vessel/transducer geometry, and this flexibility makes it useful for validating or calibrating blood flow measurement systems under a wide variety of conditions similar to those found in the human body.

ACKNOWLEDGMENT

The authors wish to acknowledge Prof. M. E. Clarke for assistance with the pulsatile pump; to P. E. Embree, B. McNeil, V. Suorsa, R. Fish, and to the reviewers for excellent comments and suggestions.

REFERENCES

- [1] S. G. Foster, P. M. Embree, and W. D. O'Brien, Jr., "Flow velocity profile via time domain correlation: error analysis and computer simulation," *IEEE Trans. Ultrason. Ferroelec. Freq. Contr.*, vol. 37, no. 3, pp. 164-175, 1990.
- [2] P. M. Embree and W. D. O'Brien, Jr., "Volumetric blood flow via time-domain correlation: experimental verification," *IEEE Trans. Ultrason. Ferroelec. Freq. Contr.*, vol. 37, no. 3, pp. 176-189, 1990.
- [3] W. R. Milnor, *Hemodynamics*. Baltimore: Williams and Wilkins, 1989.
- [4] W. W. Nichols and M. F. O'Roarke, *McDonald's Blood Flow in Arteries*. Philadelphia: Lea and Febiger, 1990.
- [5] A. J. Vander, J. H. Sherman, and D. S. Luciano, *Human Physiology*. New York: McGraw Hill, 1980.
- [6] Y. Douville, K. W. Johnston, M. Kassam, P. Zuech, R. S. C. Cobbold, and A. Jares, "An in-vitro model and its application for the study of carotid Doppler spectral broadening," *Ultrasound Med. Biol.*, vol. 9, no. 4, pp. 347-356, 1983.
- [7] W. F. Voyles, S. A. Altobelli, D. C. Fisher, and E. R. Greene, "A comparison of digital and analog methods of Doppler spectral analysis for quantifying flow," *Ultrasound Med. Biol.*, vol. 11, no. 5, pp. 727-734, 1985.
- [8] Y. W. Yuan and K. K. Shung, "Echogenicity of whole blood," *J. Ultrasound Med.*, vol. 8, pp. 425-434, 1989.
- [9] Y. F. Law, K. W. Johnston, H. F. Routh, and R. S. C. Cobbold, "On the design and evaluation of a steady flow model for Doppler ultrasound studies," *Ultrasound Med. Biol.*, vol. 15, no. 5, pp. 505-516, 1989.
- [10] P. Tortoli, F. Valgimigli, G. Guidi, and P. Pignoli, "Clinical evaluation of a new anti-aliasing technique for ultrasound pulsed Doppler analysis," *Ultrasound Med. Biol.*, vol. 15, no. 8, pp. 749-756, 1989.
- [11] B. Lavandier, D. Cathignol, R. Muchada, B. B. Xuan, and J. Motin, "Noninvasive aortic blood flow measurement using an intraesophageal probe," *Ultrasound Med. Biol.*, vol. 11, no. 3, pp. 451-460, 1985.
- [12] Y. F. Law, R. S. C. Cobbold, K. W. Johnston, and P. A. J. Bascom, "Computer-controlled pulsatile pump system for physiological flow simulation," *Med. Biol. Eng. Comp.*, vol. 25, pp. 590-595, 1987.
- [13] J. N. Peterson, "Digitally controlled system for reproducing blood flow waveforms in vitro," *Med. Biol. Eng. Comp.*, vol. 22, pp. 277-280, 1984.
- [14] W. N. McDicken, "A versatile test-object for the calibration of ultrasonic Doppler flow instruments," *Ultrasound Med. Biol.*, vol. 12, no. 3, pp. 245-249, 1986.
- [15] P. R. Hoskins, T. Anderson, and W. N. McDicken, "A computer controlled flow phantom for generation of physiological Doppler waveforms," *Phys. Med. Biol.*, vol. 34, no. 11, pp. 1709-1717, 1989.
- [16] M. M. Werneck, N. B. Jones, and J. Morgon, "Flexible hydraulic simulator for cardiovascular studies," *Med. Biol. Eng. Comp.*, vol. 22, pp. 86-89, 1984.
- [17] J. K. Poots, K. W. Johnston, R. S. C. Cobbold, and M. Kassam, "Comparison of CW Doppler ultrasound spectra with the spectra derived from a flow visualization model," *Ultrasound Med. Biol.*, vol. 12, no. 2, pp. 125-133, 1986.
- [18] A. P. Shortland and T. Cochrane, "Doppler spectral waveform generation in vitro: an aid to diagnosis of vascular disease," *Ultrasound Med. Biol.*, vol. 15, no. 8, pp. 737-748, 1989.
- [19] D. W. Holdsworth, D. W. Rickey, M. Drangova, R. Frayne, D. J. M. Miller, and A. Fenster, "A computer-controlled pump for Doppler flow calibration," *J. Ultrasound Med.*, vol. 10, no. 3 (Supplement). Official Proceedings 35th Annual AIUM Convention, S13, 1991.
- [20] D. P. Giddens and A. M. A. Khalifa, "Turbulence measurements with pulsed Doppler ultrasound employing a frequency tracking method," *Ultrasound Med. Biol.*, vol. 8, no. 4, pp. 427-437, 1982.
- [21] D. N. Ku, D. P. Giddens, D. J. Phillips, and D. E. Strandberg, Jr., "Hemodynamics of the normal human carotid bifurcation: In vitro and in vivo studies," *Ultrasound Med. Biol.*, vol. 11, no. 1, pp. 13-26, 1985.
- [22] I. A. Hein and W. D. O'Brien, Jr., "Volumetric measurement of pulsatile flow via ultrasound time-domain correlation," *Cardiovascular Technol.*, vol. 8, no. 4, pp. 339-348, 1989.
- [23] I. A. Hein, V. Suorsa, J. Zachary, R. Fish, J. Chen, W. K. Jenkins, and W. D. O'Brien, Jr., "Accurate and precise measurement of blood flow using ultrasound time-domain correlation," in *IEEE 1989 Ultrasonics Symp. Proc.*, Montreal, Canada, 1989, pp. 881-886.
- [24] I. A. Hein, "Measurement of volumetric blood flow using ultrasound time-domain correlation," Ph.D. dissertation, Dept. of Elect. Eng., Univ. Illinois at Urbana-Champaign, 1991.
- [25] V. L. Streeter, *Fluid Mechanics*. New York: McGraw-Hill, 1971.
- [26] *Operating Manual for SWF-SRD Electromagnetic Square Wave Flowmeter*. Zepeda Instruments, Seattle, WA, 1987.
- [27] B. Alberts, D. Bray, J. Lewis, M. Raff, K. Roberts, and J. D. Watson, *Molecular Biology of the Cell*. New York: Garland, 1983.
- [28] W. R. Brody and J. D. Meindl, "Theoretical analysis of the CW Doppler ultrasonic flowmeter," *IEEE Trans. Biomed. Eng.*, vol. BME-21, pp. 183-192, Mar. 1974.
- [29] B. A. J. Angelson, "A theoretical study of the scattering of ultrasound from blood," *IEEE Trans. Biomed. Eng.*, vol. BME-27, pp. 61-67, Feb. 1980.
- [30] P. R. Hoskins, T. Loupas, and W. N. McDicken, "A comparison of the Doppler spectra from human blood and artificial blood used in a flow phantom," *Ultrasound Med. Biol.*, vol. 16, no. 2, pp. 141-147, 1990.



Ilmar A. Hein (S'90-M'90) was born in Woodstock, IL, on August 15, 1959. He received the B.S., M.S., and Ph.D. degrees in electrical engineering from the University of Illinois at Urbana-Champaign in 1981, 1983, and 1990, respectively.

From 1983 to 1985 he worked as a microwave engineer at Hughes Aircraft Company in El Segundo, CA. He is currently a postdoctoral research associate at the University of Illinois where his interests include signal processing, ultrasonic

measurement of blood flow and tissue motion by time-domain correlation methods, and other bioengineering projects.

Dr. Hein is a member of IEEE, the Acoustical Society of America (ASA), and the American Institute of Ultrasound in Medicine (AIUM). He was awarded the Terrence Matzuk Memorial Award by AIUM for innovative research in the development of ultrasonic instrumentation and technology in 1988.



William D. O'Brien, Jr. (S'64-M'70-SM'79-F'89) was born in Chicago, IL, on July 19, 1942. He received the B.S., M.S., and Ph.D. degrees from the University of Illinois, Urbana, in 1966, 1968, and 1970, respectively.

From 1971 to 1975 he was with the Bureau of Radiological Health (currently the Center for Devices and Radiological Health) of the U.S. Food and Drug Administration. Since 1975 he has been at the University of Illinois where he is a Professor of Electrical and Computer Engineering and

of Bioengineering, College of Engineering, and Professor of Bioengineering, College of Medicine. His research interests involve the many areas of ultrasound-tissue interaction, including spectroscopy, risk assessment, biological effects, tissue characterization, dosimetry, blood flow measurements, and acoustic microscopy, for which he has published over 100 papers.

Dr. O'Brien is Editor-in-Chief of the *IEEE TRANSACTIONS ON ULTRASONICS, FERROELECTRICS, AND FREQUENCY CONTROL*. He is a Fellow of the Acoustical Society of America and the American Institute of Ultrasound in Medicine (AIUM) and was the recipient of an IEEE Centennial Medal (1984), the AIUM Presidential Recognition Award (1985), and the IEEE Outstanding Student Branch Counselor Award (1989). He was President (1982-1983) of the IEEE Sonics and Ultrasonics Group (currently the IEEE Ultrasonics, Ferroelectrics, and Frequency Control Society), Co-Chairman of the 1981 IEEE Ultrasonics Symposium and General Chairman of the 1988 IEEE Ultrasonics Symposium. He was also the President of the AIUM (1988-1991). He is on the Editorial Boards of the *Journal of Ultrasound in Medicine*, *Journal of Cardiovascular Technology*, and *Journal of Diagnostic Medical Sonography*.